Transportation Research Part D 115 (2023) 103580

Contents lists available at ScienceDirect

Transportation Research Part D

journal homepage: www.elsevier.com/locate/trd

Role of vehicular emissions in urban air quality: The COVID-19 lockdown experiment

Maider Llaguno-Munitxa [a,*], Elie Bou-Zeid [b]

[a] Faculty of Architecture, Architectural Engineering and Urban Planning, UCLouvain, Place du Levant 1, 1348 Ottignies-Louvain-la-Neuve, Belgium
[b] Department of Civil and Environmental Engineering, Princeton University, Princeton, NJ, USA

ARTICLE INFO

Keywords:
Urban Air Pollution
Urban Vehicular Emissions
Vehicle Electrification
Emerging Mobility
COVID-19 Lockdown

ABSTRACT

While the decrease in air pollutant concentration during the COVID-19 lockdown is well documented, neighborhood-scale and multi-city data have not yet been explored systematically to derive a generalizable quantitative link to the drop in vehicular traffic. To bridge this gap, high spatial resolution air quality and georeferenced traffic datasets were compiled for the city of London during three weeks with significant differences in traffic. The London analysis was then augmented with a *meta*-analysis of lower-resolution studies from 12 other cities. The results confirm that the improvement in air quality can be partially attributed to the drop of traffic density, and more importantly quantifies the elasticity (0.71 for NO_2 & 0.56 for $PM_{2.5}$) of their linkages. The findings can also inform on the future impacts of the ongoing shift to electric vehicles and micro-mobility on urban air quality.

1. Introduction

The SARS-CoV-2 pandemic has transformed the world. The lockdown policies, which have been frustrating for citizens and devastating for local economies, have on the other hand proved very beneficial for the environmental health of the planet (European Environment Agency 2021a, 2021b). The reduced industrial activities and vehicular and aerial traffic of goods and passengers imposed in various countries have given us unprecedented opportunities to understand the impact of anthropogenic activities on environmental health. This is particularly the case for cities where the lockdown measures have been most strict. An important question is whether this forced experiment can help us accelerate the decoupling of human activities and economic growth from resource use and pollutant emission, and promote urban planning strategies for urban health (Oke et al., 2017).

Well over a hundred papers have already been published in the past two years reporting substantial improvements of air quality conditions induced by the COVID-19 restrictions. Making use of national air quality station networks and remote sensing datasets, most of the prior literature has focused on the study of national, regional or metropolitan air quality conditions before and after COVID-19 measures started to be put in place. Reductions in atmospheric concentrations were reported to be different for distinct pollutants; however, prior literature generally agreed that the traffic-related NO_2 suffered the biggest drop, with less consistent but still significant drops also observed for $PM_{2.5}$ (European Environment Agency 2021a, 2021b; Chossiere et al., 2021; Venter et al., 2020). Prior literature also reported strong variations between regions, and cities. A study focusing on 5 megacities in India reported a $PM_{2.5}$ reduction between the studied cities ranging between 10 and 62 % (Ravindra et al., 2021). Heterogeneous contaminant concentration

* Corresponding author.
E-mail address: maider.llaguno@uclouvain.be (M. Llaguno-Munitxa).

https://doi.org/10.1016/j.trd.2022.103580
Received 11 July 2022; Received in revised form 17 November 2022; Accepted 18 December 2022
Available online 22 December 2022
1361-9209/

drops have also been observed depending on the travel restriction policies applied in different regions and urban areas in China (Wang et al., 2021a, 2021b; Gao et al., 2021; Chen et al., 2021; Le et al., 2020). Numerous publications have reported drops in the airborne contaminant concentrations to be attributable to the decrease in the number of combustion vehicles for cities such as Milan, Prague, Madrid, Paris or London (Carcel-Carrasco et al., 2021). Quantitatively, a study in Southern Italy attributed a ∼ 30 % reduction in the NO_2 concentration levels to COVID-19 related restrictions, which reduced vehicular traffic by ∼ 80 % at the city scale (Marinello 2021). Another study developed in a Southern region in Spain reported ∼ 50 % reduction in NOx related to limitations in road traffic (Cerrato-Alvarez et al., 2021). In Budapest, a reduction of 50 % in the traffic was linked to a reduction of contaminant concentrations in different phases during the pandemic, with the highest drop of ∼ 50 % for NO_2 (Salma et al., 2020). Studies combining surface and remote sensing NO_2 concentrations for the city of Rome reported reductions of 50 % for inter-urban stations, 34 % for suburban stations, and 20 % for rural stations (Bassani et al., 2021). Utilizing datasets collected from intra-urban air quality stations, comparisons of air contaminant concentrations prior and following the COVID-19 lockdown measures have also been developed for cities such as Delhi, where highest air pollution reductions were observed in areas with high transportation and industrial activities (Sahoo et al., 2021).

Augmenting the above referenced city-scale station studies, some recent investigations have used more local experimental datasets recorded by individual urban and suburban air quality stations and local traffic control datasets. This is the case for example of a study developed using datasets collected by a station neighboring a highway in Seattle to compare pre-pandemic and post-pandemic concentration values for NO_x and $PM_{2.5}$, and the concomitant traffic change. This study reported median traffic volume reductions of up to ∼ 37 %, which were associated with contaminant concentration reductions of 33 % for $PM_{2.5}$ and 30 % for NO_2 (Xiang et al., 2020). A study in California also investigated near road concentrations and their relation to the drop in the traffic at a regional scale using near-road air pollution data from the U.S. Environmental Protection Agency's AirNow database. This study reported a decline in traffic of ∼ 25 % and between 15 % and 29 % reduction for NO_2 for Northern and Southern California respectively (Liu et al., 2021a, 2021b). A recent study in Shanghai reported a direct relationship between the drop in traffic related pollutants and highlighted substantial differences between the roadside and non-roadside stations where primary pollutants dropped 34–48 % at roadside stations, and 18–50 % at non-roadside stations (Wu et al., 2021). Another source of measurements are the high spatio-temporal resolution datasets collected through low-cost sensor network and mobile sensing strategies, which are becoming increasingly popular for capturing intra-urban air quality gradients (Motlagh et al., 2021; Llaguno-Munitxa and Bou-Zeid, 2020a, 2020b; Yang and Bou-Zeid 2019; Apte et al., 2017). Various studies have made use of these datasets and reported that lockdown measures have revealed heterogeneous drops of air pollution at the neighborhood level and have been associated with reference traffic volume reductions (Chadwick et al., 2021; Wang et al., 2021a, 2021b; Hudda et al., 2020).

In this recent but extensive prior literature, the influence of traffic on regional and city scale air pollution concentrations during the COVID-19 lockdowns has been documented; with expected results. What remains missing are i) high spatial resolution studies that reveal the linkages between neighborhood scale air pollution gradients and vehicular traffic density, and ii) generalizable metrics of the sensitivity of pollutant concentrations to traffic that can be used to guide air quality management policy in various cities. This is particularly valuable given the rapid shift in urban mobility modes, the subsequent urban land use transformation, and the increasing urgency of ensuring urban environmental justice. Electrification of passenger cars and the emergence of electric micro-mobility alternatives (e-bikes, scooters, etc.) cut emissions of NO_2 (but not PM) in a very similar way to reduced gas–powered car traffic, and generalizable quantitative metrics can help policy makers project the benefits of such technological shifts for their cities (Chicco & Diana 2021; Tsakalidis et al., 2020). Such metrics can be established either using high resolution studies of a single city to measure the traffic-pollution elasticity in different neighborhoods, or they can be inferred from city-averaged data of multiple metropolitan areas. Prior studies have mainly focused on the macro (city to regional) scale studies, while neighborhood scale studies remain limited.

This study combines both of these approaches, to the best of our knowledge, for the first time in the published literature. A neighborhood to city-scale study was conducted in London that makes use of direct–sensing air pollution datasets (for NO_2 and $PM_{2.5}$), together with local traffic count datasets, at high spatio-temporal resolutions from weeks prior and following COVID-19 lockdowns. This allows measuring the intra-urban gradients of air pollution and how they are modulated by vehicular emissions. Similar datasets are increasingly available for many cities around the globe, but have not yet been utilized to their full potential. To further support this local-scale analysis, a *meta*-dataset at the city scale from the recent literature for 12 other cities was constructed, providing further support to the quantitative links between traffic and air quality, again focusing on NO_2 and $PM_{2.5}$. A primary goal is to segregate the traffic related improvements in air quality from other drivers such as reduced commercial building heating or restaurant activity.

2. Local and broader contexts and emission sources

The high-resolution analyses in the present paper focus on the influence of traffic on NO_2 and $PM_{2.5}$ concentrations in the city of London. Air quality has been a central focus for the Mayor's office of London in the last few years. Air quality policies and plans that have been included in the healthy street initiative (Mayor of London 2017), have influenced traffic restriction policies such as the implementation of the Ultra-Low Emissions Zone (ULEZ), or the partnership with the C40 Cities Climate Leadership, which led to the development of the Breathe London Project (Breathe London 2022, 2020; Environmental Defense Fund 2020). The acknowledgement of socio-demographic and environmental inequity has also been critical for the city given reports that COVID-19 related fatality rates and air pollution levels were shown to be highly correlated, revealing the differing risks of exposure based on the borough (Sasidharan et al., 2020). The mayor's office has also recently reported a drop in air contaminant concentrations of ∼ 60 % due to COVID-19 related restrictions (City of London 2021).

However, identifying the fraction of the contaminant concentrations that are directly attributable to local on-road emissions can be very challenging. NO_2 is a primary pollutant that is most often emitted through combustion sources such as motor vehicles, buildings, ships, or construction machinery into the air, and, to a lesser extent, can also be formed as a secondary pollutant through oxidization (Seinfeld & Pandis, 2006). $PM_{2.5}$ on the other hand, while also directly emitted from on-road vehicles, is significantly boosted by secondary formation from other pollutants including SO_2, NO_x, NH_3 or VOC. Most importantly, for a given location, the fraction of $PM_{2.5}$ that has been transported versus locally released by on-road vehicles will very much depend on the environmental conditions and may not be directly linkable to the local vehicular exhaust (Liu et al., 2021a, 2021b, Timmers and Achten, 2016). This explains the high variability - ranging from 20 % to 80 % - in the ratios of secondary formation of $PM_{2.5}$ (Hodan & Barnard 2004). As indicated by Monks (2012), unlike NO_2, $PM_{2.5}$ often comes from regional and transnational origins.

For the particular case of London, it is estimated that nearly half of the $PM_{2.5}$ contaminant concentration is not locally generated (Greater London Authority 2019, 2020). Thus, as described in the reports published by the office of the Mayor of London, in order to aim for a substantial improvement of the air quality in the city, regional and transnational measures will also need to be implemented. This results in uncertainties, including in the present study, in the attribution of the $PM_{2.5}$ contaminant concentration. Therefore, direct linkages between traffic and NO_2 concentration reduction may be more robust than for $PM_{2.5}$. However, as for NO_2, the most important local sources of $PM_{2.5}$ concentrations in London are connected to the transportation systems (Greater London Authority 2019, 2020). This is the reason why the reduction of on-road emissions has been, since 2016, one of the most important projects for the city. Measures such as the implementation of fully electric London black cabs and bus electrification, amongst others, are already being introduced.

To that end, the present research makes use of the extensive air quality datasets collected by the city's Breathe London project (Breathe London 2020), and TomTom traffic datasets (TomTom 2021). Given the mobility restrictions imposed in the city due to the spread of the COVID-19 pandemic, studying air quality and traffic datasets from pre-lockdown and post-lockdown weeks provided this research with the framework to evaluate the effect of the restrictions on traffic in distinct areas in the city. Aside from the impact of decreased traffic volume in the reduction of contaminant concentration, many papers have also reported the critical role meteorological conditions play in the understanding of these relations (Gkatzelis et al., 2021; Xiang et al., 2020). Thus, this paper also makes use of high spatio-temporal datasets of traffic, air quality, and meteorological parameters (wind velocity, wind direction, air temperature, and humidity, radiation, and precipitation) for the city of London, and for three weeks before and after the lockdown measures were implemented. The aim is to ensure that the findings we report are attributable to decreased traffic, rather than meteorological variability.

3. Materials and methods

This research utilized the air quality data collected through the Breathe London air quality survey developed from 2018 to 2020. The Breathe London air quality monitoring network is a consortium composed by local municipal institutions, and led by the Environmental Defense Fund Europe (EDF Europe). The initiative followed the implementation of the worlds' first Ultra Low Emission Zone (ULEZ) in Central London. Using a low-cost air quality sensing kit (sensors models, specs, and performance tests available at (AQMesh 2022)), the key ambition of the Breathe London project was to characterize the spatial patterns of air pollution across the city to assess

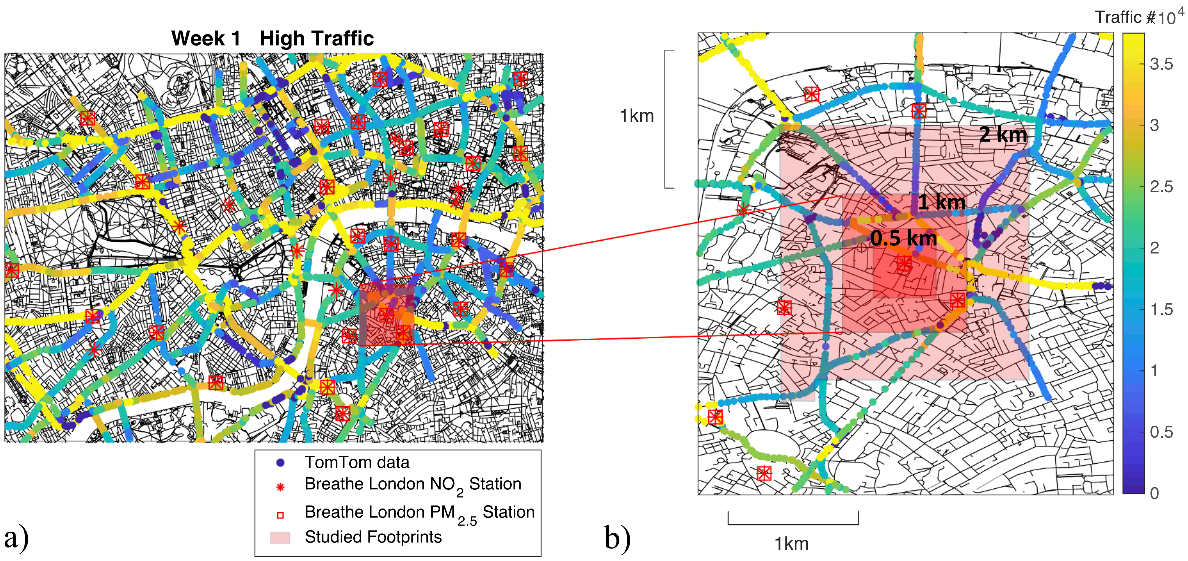

Fig. 1. Breathe London Station Location and Footprint Method Display a) Traffic count data collected from TomTom for week 1 - High Traffic. The red stars display the location of the Breathe London NO_2 stations located within the City of London, and the red boxes display the location of the $PM_{2.5}$ stations b) example of the studied three footprint sizes d = 0.5 km, d = 1 km and d = 2 km. (For interpretation of the references to color in this figure legend, the reader is referred to the web version of this article.)

policy interventions. As part of the Breathe London project, 3 sensing campaigns (stationary, mobile and citizen-led) were developed; however, the work presented in this paper has solely used the data collected by the stationary network, which included ~ 100 sensor pods installed across the city of London (Breathe London 2020). The ~ 100 stations collected data for two pollutants: fine particulates, and nitrogen oxides. The datasets were made available at hourly temporal resolution. With the aim to characterize the pedestrian level concentrations, the Breathe London air quality stations were installed on lamp posts and facades at ~ 3 m heights. Positioning the sensing kits in close proximity to the vehicular emissions, as opposed to on rooftops or non-urban environments where traditional regulatory stations were placed, is critical to better capture the on-road emissions. Long-range transported NO_2 and $PM_{2.5}$ concentrations and most building emissions will have to be diffused by turbulent and dispersive fluxes into the urban canopy layer and then to the pedestrian level (Li & Bou-Zeid 2019, Llaguno-Munitxa & Bou-Zeid 2018), while traffic emissions will be in the direct vicinity of these stations. The Breathe London campaign focused on the NO_x and $PM_{2.5}$ air contaminants released through burning of fossil fuels

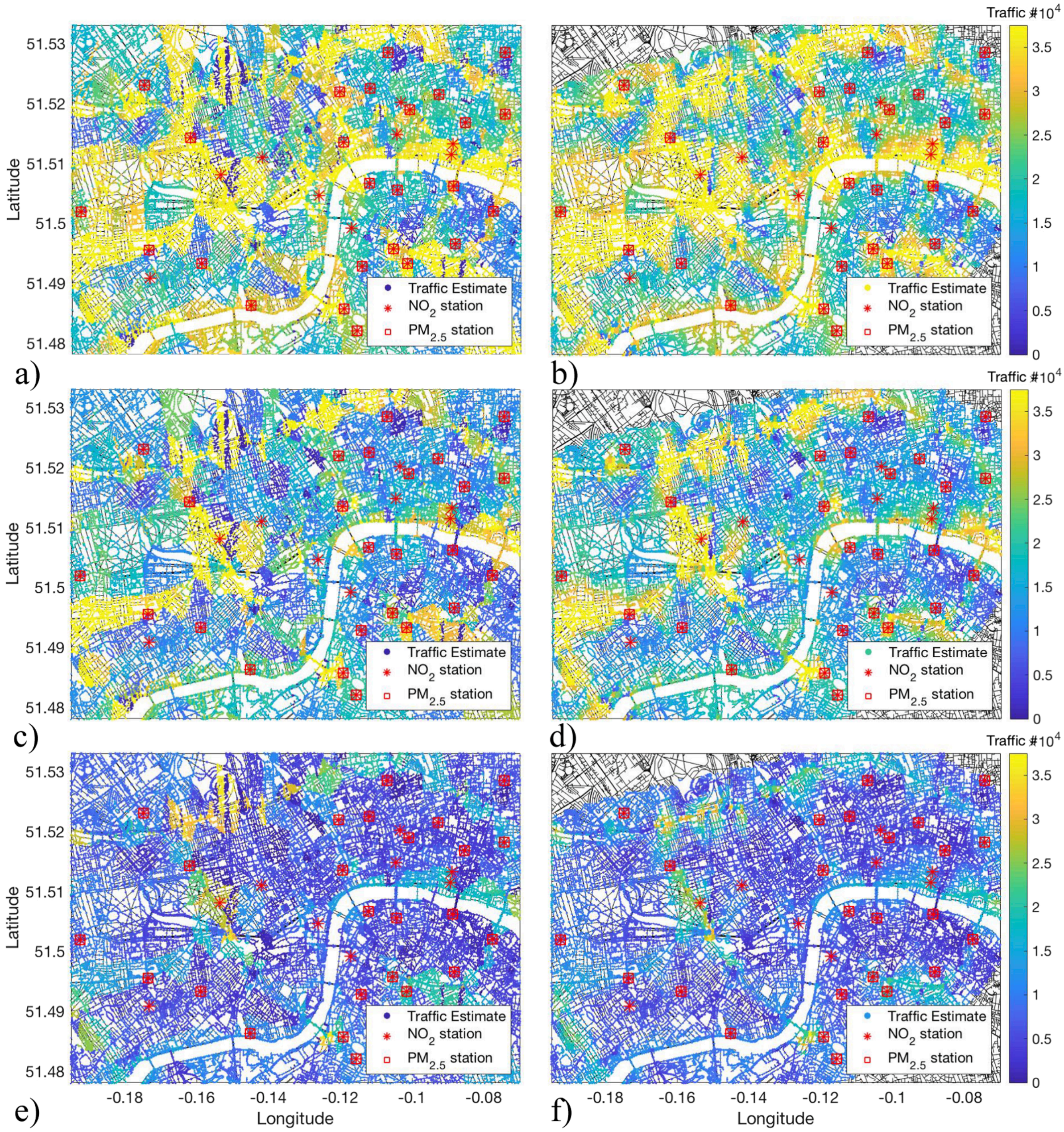

Fig. 2. Display of the traffic count estimations using Method #1 and Method #2 based on the TomTom data. a) Week #1- High Traffic- traffic estimation using Method #1. b) Week #1- High Traffic- traffic estimation using Method #2. c) Week #2- Intermediate Traffic- traffic estimation using Method #1. d) Week #2- Intermediate Traffic- traffic estimation using Method #2. e) Week #3- Low Traffic- traffic estimation using Method #1. f) Week #3- Low Traffic- traffic estimation using Method #2.

such as diesel and petrol vehicles, or gas-powered heating for homes and businesses. In a recent summary of the Breathe London project, it has been reported that an average NO_2 concentration reduction of 17–24 % took place across the full Breathe London network at Greater London, and 28–30 % in the Breathe London network located in the City of London ULEZ boundary (Breathe London 2020; Environmental Defense Fund 2020) during the course of the project. Fig. 1a displays the locations of the Breathe London subset of stations studied in this paper, which are located within the City of London.

High spatiotemporal air quality datasets have been collected for 3 weeks. The selection of the weeks follow the dates before and after the UK lockdown, which took place on the 26th of March, to capture the effect of the lockdown on the vehicular traffic density in the city. Week #1 from March 2nd 2020 until the 8th of March captures the characteristic traffic concentration in a usual pre-COVID-19 scenario, Week #2 from the 16th of March until the 22nd of March captures the situation of a reduced traffic scenario when the population where starting to understand that a lockdown was about to be imposed, Week #3 from the 30th of March until the 5th of April was the second week post lockdown when the traffic density was lowest. Week #1 is also labeled as High Traffic, Week #2 as Medium Traffic, and Week #3 as Low Traffic in the paper. The air quality datasets have been obtained from the Breathe London server for NO_2 and $PM_{2.5}$ at hourly intervals for $\sim$ 100 stations distributed across the greater London metropolitan area. From all stations, only the $\sim$ 25 stations located within the city of London have been used for the analyses of this paper (see Fig. 1).

Provided the spatial resolution of the air quality network of the Breathe London project, traffic data at a comparable spatial resolution was sought using TomTom data (TomTom 2022). From the TomTom Move portal, georeferenced vehicular traffic count data were collected for the three weeks of study. TomTom provides traffic count data per road segment and thus the utilized datasets offer a high spatial resolution representation of the traffic gradients in the city. As shown in Fig. 1a, the TomTom traffic volume count data were collected solely for the main road arteries located in the city of London. Weekly averaged traffic count data were collected for the selected weeks. While biases were reported in the TomTom traffic volume data (Gensheimer et al., 2021), this paper mainly seeks to quantify the change in traffic, and for such differences the impact of biases would be reduced. The study presented in this paper has focused on the city of London area where $\sim$ 25 Breathe London stations are located (see Fig. 1). For every-one of these stations a data quality control process was applied.

3.1. Statistical analysis

For all stations and using the hourly data, an outlier replacement filter was applied where the values larger than three scaled median absolute deviations from the local median, defined by $\pm$ 3 h, were replaced by the nearest value. A spatial filtering was also deployed, for every hour and for all stations in the city, where the values outside the [3–97] percentiles were replaced by the city mean value for that given hour. Once the data had been processed, the mean and standard deviation were computed for all 3 weeks.

For each air quality station, traffic count metrics have been computed following a traffic estimation model.

TomTom provides the traffic volume counts per road segment and given that these segments do not spatially coincide with the Breathe London station locations, the traffic counts in the Breathe London stations were estimated following two methodologies. In Method #2, the traffic data were interpolated using a triangulation-based linear method to generate a 25 m $\times$ 25 m resolution map of traffic count. Given that the total traffic counts need to be estimated for each Breathe London station, the 25 m traffic count data is referred to each station as $T_{i,25}$, where the index i $\in$ [1, 25] denotes the station. In order to obtain the traffic count estimate for each station location, a footprint-based study was adopted where the neighborhood scale traffic count is captured at different scales around the station (Llaguno-Munitxa et al., 2021; Llaguno-Munitxa and Bou-Zeid, 2020a, 2020b) As displayed in Fig. 1.b, footprints of 0.5 km $\times$ 0.5 km, 1 km $\times$ 1 km and 2 km $\times$ 2 km were assessed. Thus, the traffic count for each footprint size was computed as T_{ij}, where j $\in$ [500 m, 1000 m, 2000 m] is the index for the footprint size. T_{ij} is obtained by averaging over the cells of $T_{i,25}$ located within the footprint for each station. The last step is to multiply the mean traffic count T_{ij} for each footprint of each station by the total road length RL_{ij} for that footprint. For Method #1 on other hand, the interpolation step was not incorporated. In this case, for each road segment located in the city of London, the nearest traffic count value available from the available TomTom data was imposed. The subsequent steps are the same as per Method #2. Fig. 2 displays the maps obtained through the study using both methods for all studied weeks. The results for both methods and three footprints have been compared by calculating their Pearson correlation coefficient (Pearson 1895) relative to the results using Method #2 for the traffic estimation and 1 km $\times$ 1 km footprint size. For all cases p-values remained $<$ 0.001 indicating that they yield very similar results. Given that the results observed following both methods are comparable, and that the results observed for Method #2 showed higher correlations against $PM_{2.5}$ and NO_2 (see results section) only the results obtained through Method #2 will be presented.

Prior to the application of the traffic model, the distances between the Breathe London stations and the available geo-localized TomTom traffic counts were computed. From the Breathe London stations located within the city of London, the average distance to the nearest TomTom reading was found to be below 100 m, while the maximum and minimum distances were 340 m and 5 m respectively.

As described above, the traffic model was deployed for footprint sizes ranging between 500 m and 2 km because not only the emissions in the immediate street canyon vicinity, but also the traffic emissions from neighboring streets, can influence the concentration values in the street canyon where the Breathe London sensor is located (Llaguno-Munitxa and Bou-Zeid, 2020a, 2020b). Therefore, the average distance of $\sim$ 100 m between the Breathe London stations and the TomTom sources was considered acceptable since it is significantly smaller than our analysis scale.

Meta-datasets for NO_2 and $PM_{2.5}$ concentration at the city scale from the recent literature for 12 other cities have been compiled, allowing us to provide further support to our quantitative links between traffic and air quality. For the compiled cases, as well as for the London case study developed in this paper, the elasticity measure that accounts for the relative fractional reduction (percentile reduction/100) in urban pollutant concentration resulting from a given fractional drop in traffic was computed (Nivergelt 1983).

3.2. Weather data

Weather data for all studied weeks were analyzed to understand if the meteorological conditions were comparable for all three weeks. Datasets on the wind speed, wind direction, air temperature, relative humidity, rainfall, and radiation were compiled. The data from the weather station located at the Heathrow airport were used for the study. The mean daily value series plots are included in

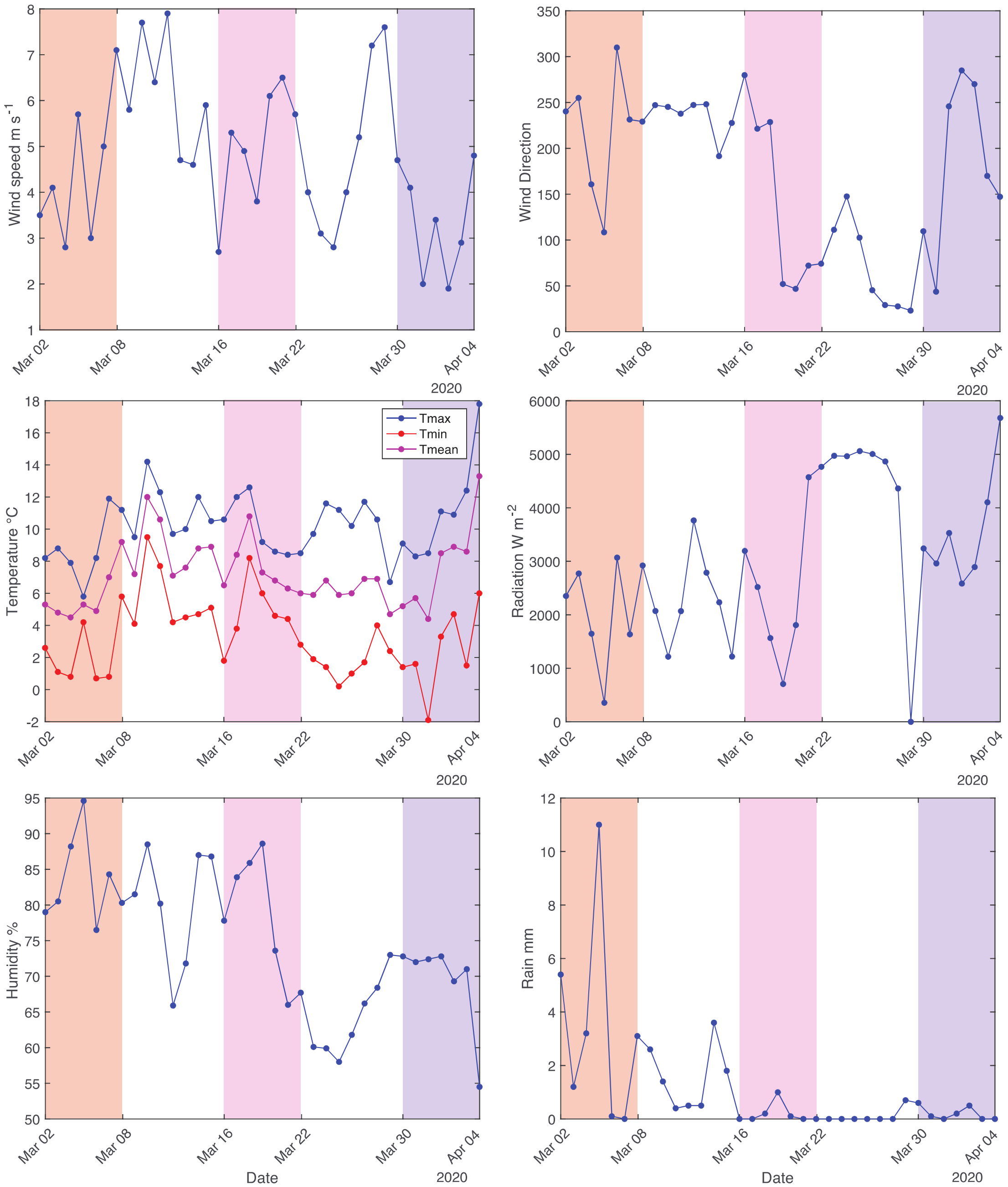

Fig. 3. Weather data collected from Heathrow airport. In the top two plots: daily average for wind velocity and wind direction. Middle row: plots for air temperature and radiation. Bottom row: plots for relative humidity and precipitation. The 3 studied weeks are highlighted using the colors orange for Week #1 – High Traffic, pink Week #2 – Medium Traffic, and purple Week #3 – Low Traffic. (For interpretation of the references to color in this figure legend, the reader is referred to the web version of this article.)

Fig. 3 for all studied weather parameters. The studied weeks are marked using three different colors, orange for Week #1, pink for Week #2 and blue for Week #3. The potential impacts of the meteorological variability on results interpretation will be discussed in the results section.

4. Results

Fig. 4a displays the daily mean concentration of NO_2 in blue, and weekly mean concentrations in red from January 1st until the 15th of August 2020, from all ~ 100 breathe London station data. The plot also displays vertical dashed lines marking the key moments related to the implementation of COVID-19 lockdown measures. The first COVID-19 lockdown in London was announced on March 23rd, and imposed on March 26th. The lockdown measures started to be lifted only after the 10th of May. On June 1st, the schools reopened, and on June 15th, the lockdown measure relaxation was announced and the non-essential shops reopened. On the 23rd of June, finally, the national lockdown came to an end. In July, some social distancing and local lockdown measures were authorized, and after the 14th of August, the COVID-19 safety restrictions were eased further. The NO_2 time series displays a reduction in NO_2 concentrations when lockdown measures were imposed. The time series plot for the contaminant $PM_{2.5}$ shown in Fig. 4b displays less identifiable trends, which is attributable to the fact that a larger percentage of $PM_{2.5}$ concentrations are transported rather than locally emitted as previously discussed. In addition, while transportation emissions of $PM_{2.5}$ were reduced during the lockdown, household emissions increased during the COVID-19 confinement period due to increased heating and food preparation in households.

Fig. 4c displays the favorable comparison of the Breathe London city mean concentration (including all ~ 100 breathe London station data) values for $PM_{2.5}$, against 2 nearby reference stations of the London Air network (Mittal 2020) located in Greenwich Etham (shown in magenta), and Westmister Marylebone (shown in red). A comparison against 4 other London Air stations located in different areas of the city was also performed, revealing similar agreement. The Pearson correlation coefficient (PCC) of the London Air reference stations mean $PM_{2.5}$ concentration, against the mean Breathe London $PM_{2.5}$ concentration remained > 0.8 ($p < 0.05$). The

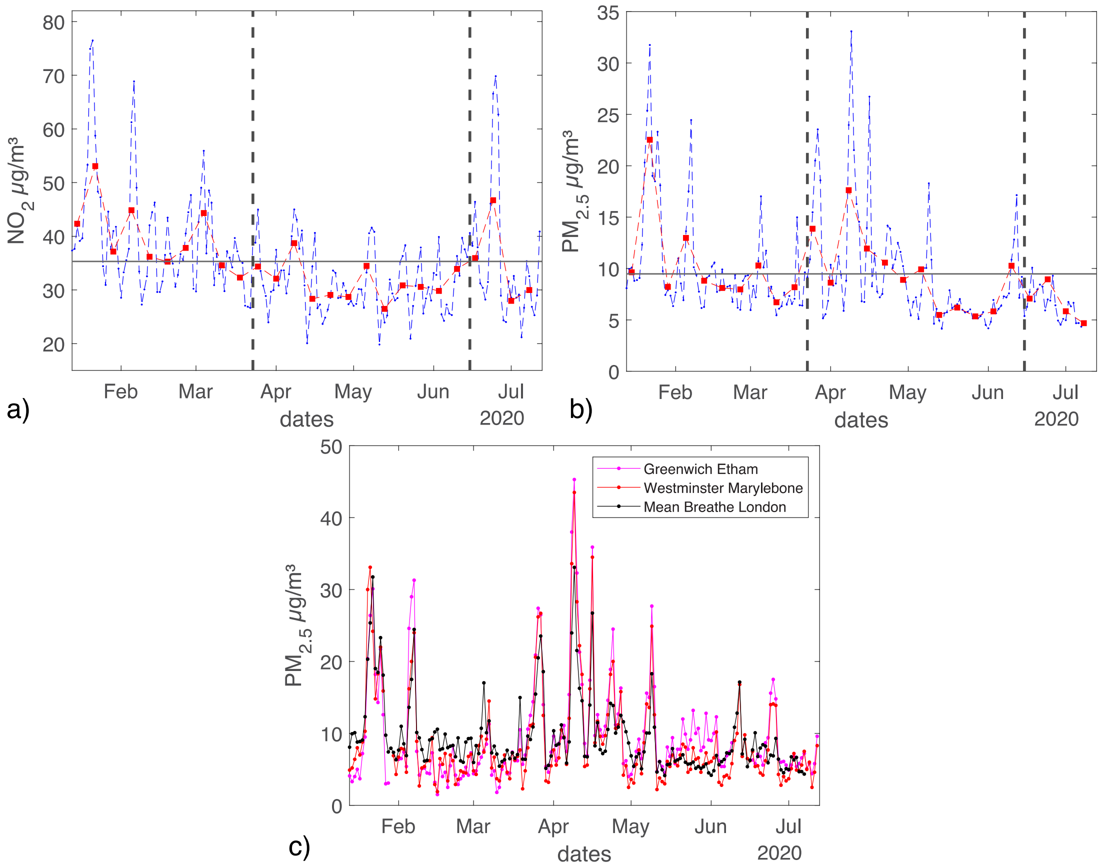

Fig. 4. Top: time series from January until August 2020 averaged across all sensors. In blue the daily mean concentration values are shown. In red the weekly mean concentration values are shown. The horizontal black line denotes the mean concentration value for the displayed period. The dotted black lines denote the lockdown beginning and lockdown restriction relaxation announcement dates a) NO_2 concentration b) $PM_{2.5}$ concentration. Bottom: figure c) time series from January until July 2020 for $PM_{2.5}$. The magenta and red lines depict the daily average time series for two London Air reference stations located in Greenwich Etham, and Westminster Marylebone. In black the time series of the Breathe London city mean is displayed. (For interpretation of the references to color in this figure legend, the reader is referred to the web version of this article.)

same study was performed for the contaminant NO_2, and slightly lower correlations were observed, between 0.65 and 0.9 ($p < 0.05$). Additionally, a comparison between the concentrations recorded by different stations of the London Air reference network was performed and it was observed that the concentration values of NO_2 between different stations were more variable than those of $PM_{2.5}$, denoting the contribution of the transported $PM_{2.5}$ contaminants (more homogeneous effect over the city) against the predominant role of locally (and more variably) emitted NO_2 contaminants.

From the collected NO_2 and $PM_{2.5}$ concentration data, 3 weeks of data have been selected for a focused study. The focus now will be on the spatial analysis of weekly-averaged data. The weekly averaging helps reduce the impact of other sources of variability including meteorological, diurnal, and weekday versus weekend effects. This then helps to isolate the effect of traffic, The histogram plots for the NO_2 and $PM_{2.5}$ concentrations in London for the studied Week #1: High traffic, Week #2: Medium traffic, and Week #3: Low traffic volume are shown in Fig. 5. The top row displays the histograms for the mean concentration values of the various stations, and the middle row displays the histograms for the temporal standard deviation at each station for the different weeks. The results show a reduction in both NO_2 and $PM_{2.5}$ mean values between the studied weeks. The largest differences are observed between Week #1 and Week #3, and only subtle differences are generally observed between Week #2 and Week #3. This is expected given that although the lockdown was not imposed until after Week #2, the traffic had already substantially reduced by then. The mean concentration for NO_2 for Week #1 was 43.94 μg/m$^{3.}$ and 32.28, and 31.84 μg/m^3 for Week #2 and Week #3 respectively. For $PM_{2.5}$, for Week #1 the mean

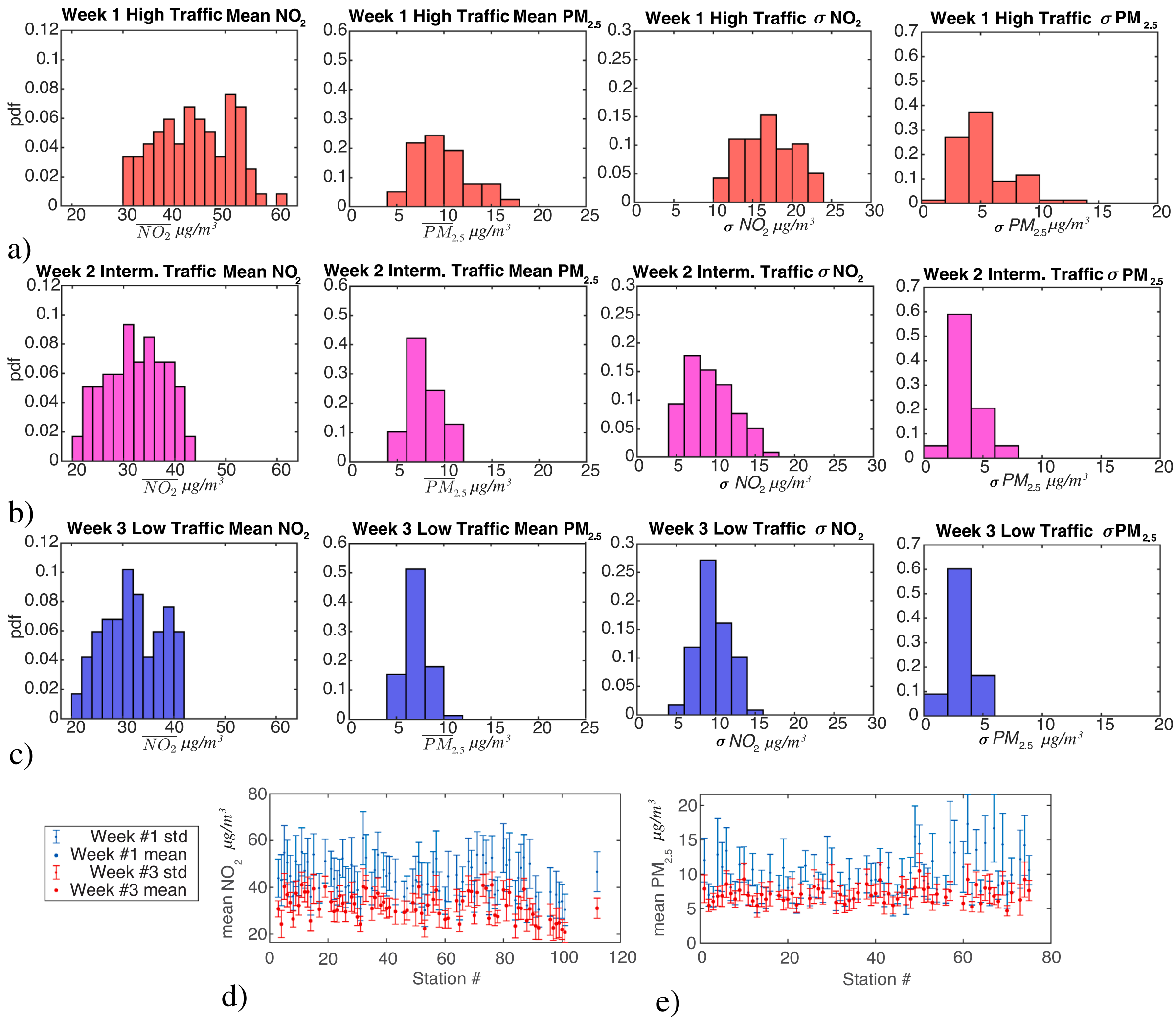

Fig. 5. Histogram of the three studied weeks using data from all stations over the London metropolitan area. From left to right, a) Week 1 High Traffic: mean of NO_2 concentration, mean of $PM_{2.5}$ concentration, standard deviation of NO_2 concentration, standard deviation of $PM_{2.5}$ concentration. b) Week 2 Intermediate Traffic: mean of NO_2 concentration, mean of $PM_{2.5}$ concentration, standard deviation of NO_2 concentration, standard deviation of $PM_{2.5}$ concentration. c) Week 3 Low Traffic: mean of NO_2 concentration, mean of $PM_{2.5}$ concentration, standard deviation of NO_2 concentration, standard deviation of $PM_{2.5}$ concentration. Mean concentration and temporal standard deviation plot for 2 of the studied weeks, Week #1 high traffic in blue and Week#3 low traffic in red for e) NO_2 f) $PM_{2.5}$. All units are μg/m^3. (For interpretation of the references to color in this figure legend, the reader is referred to the web version of this article.)

concentration was 9.81 μg/m^3, dropping to 7.91 and 7.10 μg/m^3 for Week #2 and Week #3 respectively. Thus, for both contaminants, a reduction of ~ 28 % has been observed. Statistically significant differences were confirmed between the studied weeks and for NO_2 and $PM_{2.5}$. The Kolmogorov-Smirnov test rejected the null hypothesis at a 5 % significance level. In addition, a large effect size (Cohen's d > 0.8) was reported through a standardized mean difference. These tests confirm that the data samples from different weeks are drawn from different distributions and significantly different from each other statistically.

For the temporal standard deviation at each station, comparable drops are observed, implying that the variation of the concentration over the course of the week was damped during lockdown. This is expected: given the higher means, higher standard deviations have also been observed for high traffic days compared to low traffic days. For the case of the $PM_{2.5}$, a positive-skew distribution can be noted, implying that very high concentrations and temporal variability are present in some stations especially during high traffic (Week 1). The NO_2 distribution on the other hand is more symmetric. In the bottom row of Fig. 5, a comparison for the mean and temporal standard deviation focusing on Week #1 and Week #3 is shown for all Breathe London stations located in Greater London and for both studied contaminants NO_2 and $PM_{2.5}$. The error bar plot displays the temporal 'hourly' standard deviation for the stations: the average temporal standard deviation for NO_2 is 17 μg/m^3 for Week #1 and 9.3 μg/m^3 for Week #3, and for $PM_{2.5}$ is 5.2 μg/m^3 for Week #1 and 3.6 μg/m^3 for Week #3. This better depicts the reduced concentration variability observed during low traffic conditions. The statistical results comparing the studied weeks and for NO_2 and $PM_{2.5}$ are also included in Table 1.

Fig. 6 displays the concentrations for NO_2 and $PM_{2.5}$ against traffic estimation (here from Method #2, see methods section) for all three studied footprints and for all 3 weeks. The two plots in the top row display the results using the traffic estimation for a footprint area of 0.5 km × 0.5 km surrounding each station, for both NO_2 and $PM_{2.5}$, those in the middle row are for the 1 km × 1 km footprint, and those in the bottom row for a footprint of 2 km × 2 km. No substantial differences are observed between the studied footprints, and a clearly positive correlation is observed between traffic and concentrations for all scales.

The proposed traffic estimation methods Method 1 and Method 2 showed comparable results for the studied footprints 0.5 km × 0.5 km, 1 km × 1 km and 2 km × 2 km, with PCC value of 0.94, 0.93, 0.73 respectively ($p < 0.05$). To quantify this relation, Table 2 shows a comparison of the obtained PCC for the studied traffic estimation methods and footprint scales. Between the tested footprint scales and traffic estimation methods, Pearson correlations show similar trends. Amongst all, the footprint scale of 2 km × 2 km area and the traffic estimation Method #2 are the ones that show highest correlations for both contaminants NO_2 and $PM_{2.5}$. It is important to underline here that concentrations are modulated by a large range of other forcings (meteorology, emissions from other sources, etc.), so these values of the correlations with a single input are in fact quite substantial (but note that emissions from other sources such as restaurants can be correlated with traffic and can be contributing to some of the trends). Regardless of the footprint scale, they confirm that the improvement of air quality can be linked to the drop of traffic density, and therefore underline the contribution of vehicular emissions to pre-COVID-19 concentrations. P-values have remained below $p < 0.05$.

Table 3 displays the city scale spatial statistics for the studied air quality and weather parameters. The spatial gradients of mean concentrations across the city of London, quantified via the spatial standard deviation (Std_s) show a more moderate reduction than their temporal counterparts, particularly for NO_2. Thus, it appears that persistent differences in the traffic volume, coupled with the spatial variability of intrinsic urban fabric characteristics, will lead to persistent spatial differences in concentrations of pollutants even when the city means are reduced significantly.

The changes in the wind direction are significant for Week #2, relative to the other two weeks. The predominant wind direction for all studied weeks comes from the South West; however, a change is observed during the second half of Week #2, when North Eastern winds prevailed. It was noted that none of the weeks had South Easterly winds that can transport significant pollutions from continental Europe and confound the analysis. All analyzed stations are located in the city center and thus it is unlikely that the change in the wind direction is going to have a very strong impact on the locally-contributed pollutant concentrations, especially given that wind velocities remained stable. The temperature is also fairly stable with a mean of ~ 8 °C except for the last two days of Week #3 when a rise in the temperature was observed. On the other hand, an important aspect to note is that Week #1 was a rainy week. Rainy days are usually associated with improved air quality conditions due to wet deposition. In addition, moderately lower wind speeds were observed for Week # 3 (increasing the pollution for this low traffic week). These meteorological influences will thus counter the effect of reduced traffic, and are thus highly unlikely to have caused the trends of variation observed in Fig. 6. In fact, without these two meteorological perturbations, a stronger correlation might have been observed.

To infer a potentially generalizable measure, the relative fractional reduction (percentile reduction/100) in urban pollutant concentration resulting from a given fractional drop in traffic was calculated; the ratio of the two is the elasticity measure often used in economic analysis (Nivergelt 1983). This metric was also computed from the data reported in 12 recent studies from various cities (at the city scale) to support our London data with a prior literature *meta*-analysis and to contextualize the presented results (Fig. 7). Bulk $PM_{2.5}$ and NO_2 contaminant drops and traffic count drops have been extracted from the prior literature that studied air quality changes from high traffic (pre-COVID-19 lock down) and low traffic (post-COVID-19 lockdown) timeframes, similarly to what is shown here for

Table 1
Statistical comparison for the 3 studied weeks (Week 1 | Pre-Lockdown, Week 2 | Mid-Lockdown, Week 3 | Post-Lockdown) for NO_2 and $PM_{2.5}$. The standard deviation value are the means of the standard deviations of all individual stations.

	Mean NO_2	Mean $PM_{2.5}$	Std NO_2	Std $PM_{2.5}$	Max NO_2	Max $PM_{2.5}$	Min NO_2	Min $PM_{2.5}$
Week 1	43.94	9.81	17.70	5.26	64.78	32.10	21.96	2.80
Week 2	32.28	7.91	9.51	3.51	47.51	15.31	12.12	2.70
Week 3	31.84	7.10	9.99	3.65	52.09	13.84	15.08	3.85

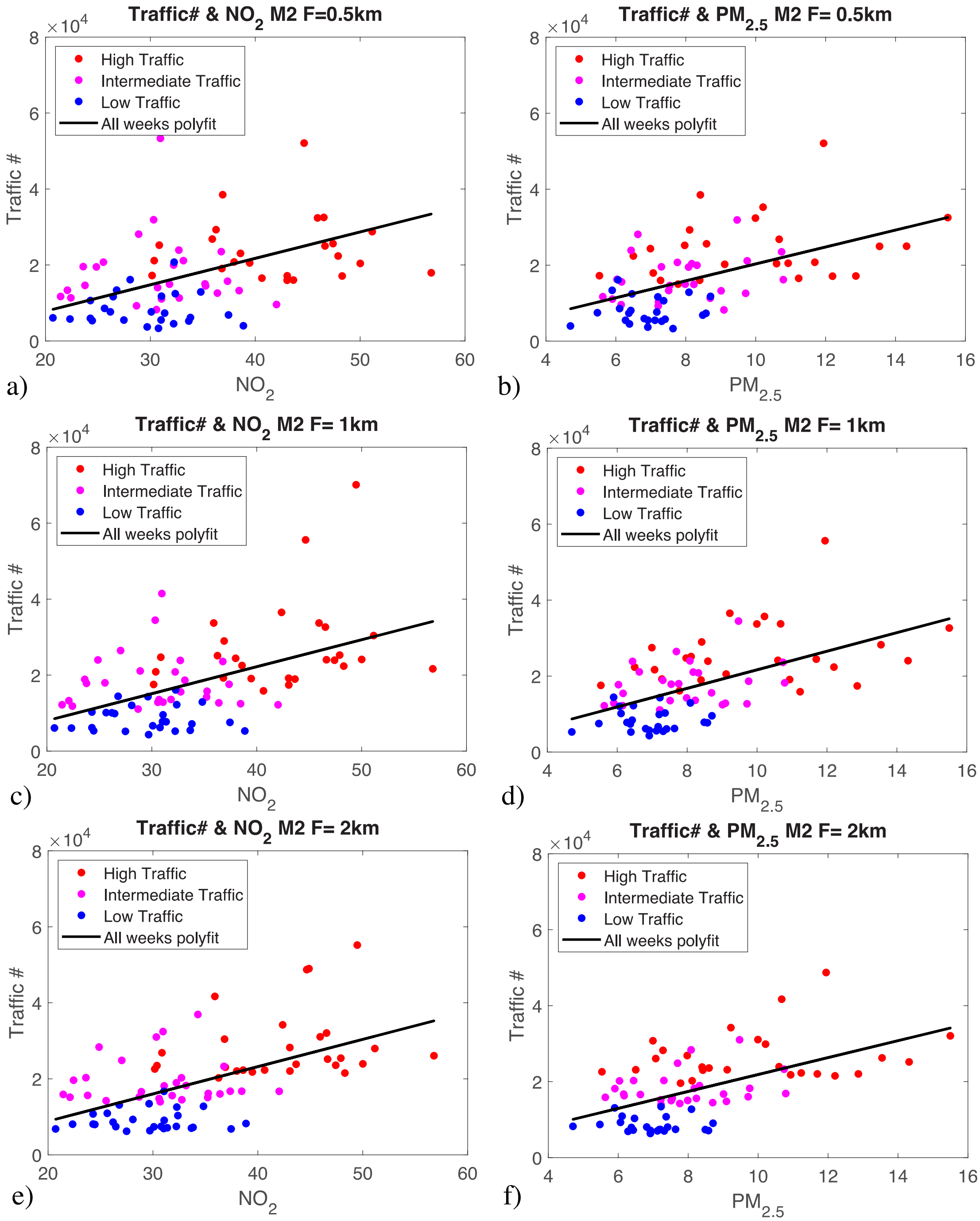

Fig. 6. Traffic count and contaminant concentration plots for distinct footprints a) c) e) Traffic estimation based on Method #2 vs NO_2 concentration for footprints 0.5 km × 0.5 km, 1 km × 1 km and 2 km × 2 km respectively b) d) f) Traffic estimation based on Method #2 vs $PM_{2.5}$ concentration for footprints 0.5 km × 0.5 km, 1 km × 1 km and 2 km × 2 km respectively. The black lines are the linear polynomial fits.

London. The results show clear trends for both pollutants with the data points often falling below the 1:1 line, which implies an elasticity < 1. Thus, a given fractional drop in traffic will not result in an equal or larger fraction drop in the pollution (as expected), but the drop will still be significant given that the mean elasticity reported here for all studies is about 0.71 for NO_2 and 0.56 for $PM_{2.5}$. It should be noted that part of the trends might be related to drops in emissions that are correlated with traffic, such as heating or industrial emissions. But the robustness of the results (small range of elasticity) across multiple cities in different climates confirms that lockdown analyses can indeed be used to infer the impact of traffic on air quality in cities, and the potential benefits of fleet electrification. The London data analyzed here also allows us to compute the half-standard deviation of the elasticity among all stations

Table 2
Comparison of PCC values for both traffic estimation methods and all footprint scales and for both contaminants NO_2 and $PM_{2.5}$.

Case	NO_2 PCC	$PM_{2.5}$ PCC
Method 1 _ Footprint 0.5 km × 0.5 km	0.41	0.41
Method 1 _ Footprint 1 km × 1 km	0.48	0.46
Method 1 _ Footprint 2 km × 2 km	0.50	0.45
Method 2_ Footprint 0.5 km × 0.5 km	0.44	0.53
Method 2_ Footprint 1 km × 1 km	0.51	0.56
Method 2_ Footprint 2 km × 2 km	0.55	0.55

Table 3
City spatial statistics for the studied air contaminant and weather parameters. For the air quality, the statistics for the central London stations have been computed. For the weather parameters, the dataset from the reference station located at London Heathrow has been used. For traffic, the estimation obtained using Method #2 and the 2 km × 2 km footprint is shown.

Parameters Stations	Mean W#1	Max W#1	Min W#1	Std_s W#1	Mean W#2	Max W#2	Min W#2	Std_s W#2	Mean W#3	Max W#1	Min W#3	Std_s W#3
$PM_{2.5}$ μg/m^3	9.81	17.31	5.05	2.85	7.91	11.58	5.09	1.65	7.10	10.04	4.70	1.16
NO_2 μg/m^3	43.94	61.01	30.17	7.42	32.28	42.30	21.44	5.75	31.84	41.08	20.71	5.65
Traffic #	27,600	55,240	19,602	8018	18,458	36,933	13,948	5301	8569	16,715	6183	2325
T °C	5.85	8.87	2.28	–	7.44	9.98	4.51	–	8.84	12.07	3.10	–
Rad W/m^2	2107	–	–	–	2733	–	–	–	3557	–	–	–
RH %	83.34	–	–	–	77.6	–	–	–	68.34	–	–	–
Precip mm	3.43	–	–	–	0.18	–	–	–	0.27	–	–	–
Wind V m/s	4.45	–	–	–	5.00	–	–	–	3.25	–	–	–
Wind D °	219	–	–	–	139	–	–	–	199	–	–	–

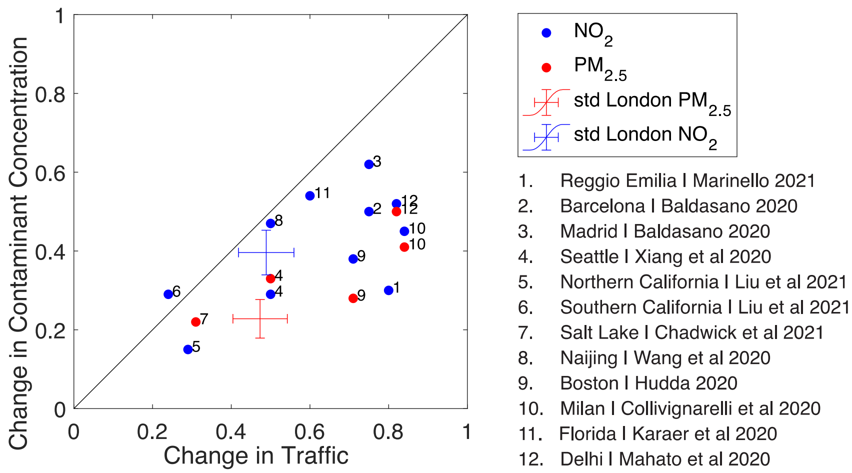

Fig. 7. meta-analysis elasticity plot displaying the fractional change in the contaminant concentration versus the change in the traffic count. The blue color depicts the data related to the contaminant NO_2 and the red color to $PM_{2.5}$. The results obtained in the study presented in the paper are shown with vertical error bars that display the ± 0.5 relative spatial standard deviation for NO_2 between Week#1 and Week#2 in the × axis in blue, and for $PM_{2.5}$ in red. The horizontal error bars display the ± 0.5 relative spatial standard deviation for the traffic count between Week#1 and Week#2. The black line is the 1:1 line corresponding to an elasticity of 1. (For interpretation of the references to color in this figure legend, the reader is referred to the web version of this article.)

(reported as error bars), showing a good agreement between the neighborhood-scale elasticities.

5. Conclusions

Making use of pre- and post-COVID-19 lockdown high spatio-temporal resolution datasets on $PM_{2.5}$, NO_2 and traffic volume, the role of vehicle emissions in the intra-urban air contaminant concentrations in the city of London was studied. The research revealed that for the studied air quality stations (~25), a drop of ~ 30 % in the contaminant concentration, with similar trends for NO_2 and $PM_{2.5}$, was observed between the weeks prior to the COVID-19 lockdown and after it was implemented in the city of London. The drop was associated with a reduction in total vehicle count between weeks preceding the lockdown and the weeks after the lockdown of ~

70 % and was generally consistent amongst all studied stations. The temporal variability of concentrations also significantly decreased at a given station, but the spatial variability drop amongst stations was more limited. As opposed to prior literature, which has mainly focused on macro scale studies, the proposed fine-resolution (~neighborhood scale) air quality concentration and traffic count data analysis has enabled the identification of inter-urban gradients and patterns.

To provide a generalizable measure of the benefits of reduced traffic emissions for cities, the elasticity was computed (fractional change in concentrations over fractional change in traffic) for each station and the whole city. Then, the London data were augmented with a *meta*-analysis of results reported over the past year for the comparable drop in concentrations in 12 other cities. The results indicate an average elasticity of about 0.71 for NO_2 and 0.56 for $PM_{2.5}$, implying a significant potential for reducing concentration in cities by simply controlling traffic emissions. These elasticities were overall reasonably consistent across the various cities, despite their distinct geoclimatic, infrastructure attributes and vehicular and heating/cooling technologies. This lends support to approaches that focus on the macro-scale similarity of cities and attempt to derive general scalings to describe their function and growth (Barthelemy 2016).

Given the recent investment of various global cities in extensive air quality networks and mobile sensing campaigns, there are opportunities to develop comparable studies at other locations to further understand if the concentrations-traffic elasticity is comparable in contexts with differing urban fabric characteristics, topographical conditions or climate. Such findings can better inform policies that aim to restrict traffic in city centers such as the Ultra-Low Emissions Zone (ULEZ) in London for the improvement of the local air quality. But they can also aid in projecting the benefits of the myriad changes in urban mobility that are underway, particularly those related to electrification and electric micro-mobility. Electric and micro vehicles reduce the direct emissions of NO_2 from traffic in cities to zero (although if the electricity is produced from fossil fuels, some emissions might be moved to other locations) since no combustion process is involved. The direct benefits for NO_2 concentration are thus comparable to those of reduced traffic. The indirect impacts related to the reactions of NO_2 and the formation of ozone are more complex since they also involve volatile organic compounds that can also be emitted from urban vegetation (Oke et al., 2017). The implications for PM concentrations are less obvious since 85 to 90 % of vehicular PM emissions are not from engine exhaust (but rather from brakes and tires) and heavier electric vehicles may increase the emissions of PM (Timmers and Achten, 2016), although regenerative braking can significantly offset and even reduce these emissions (Liu et al., 2021a, 2021b). Lighter micro vehicles would, however, significantly reduce PM emissions. Future studies should thus aim to elucidate these factors, as well as seek to include other significant sources of air pollution in cities (long range transport, heating/cooling, industrial and commercial emissions) to better isolate and quantify the impact of traffic and the benefits of electrification.

Limitations of the present study are related to the low spatio-temporal granularity of the traffic count and air quality datasets. The purchased TomTom traffic count data was averaged for each week under study, and for all road segments located in primary and secondary streets in the city of London. To increase the spatial resolution of the collected TomTom data, traffic count estimates for all streets were derived through the deployment of a traffic model. For future studies, case studies where a higher spatial resolution traffic count data is accessible could be sought. Similarly, while the Breathe London air quality network is one of the densest urban air quality networks available today, it still has limited spatial coverage and may not capture all the neighborhood scale variability for the urban gradients in air-quality. In the future, mobile sensing systems can be used to obtain more spatially representative data (Yang and Bou-Zeid 2019).

Funding

Project funding was provided by Samsung Advanced Institute of Technology under AGRMT.dtd 10–4-19, and the Army Research Office under contract W911NF2010216 (program manager Julia Barzyk).

Research Data

The raw Breath London data are available at (https://www.breathelondon.org/), while the raw traffic data from can be purchased from TomTom (https://move.tomtom.com).

All derived data used in this paper, and the corresponding codes, will be made available upon acceptance for publication at (Princeton University public data storage).

CRediT authorship contribution statement

Maider Llaguno-Munitxa: Conceptualization, Data curation, Formal analysis, Investigation, Methodology, Project administration, Resources, Software, Validation, Visualization, Writing – original draft. **Elie Bou-Zeid:** Conceptualization, Data curation, Funding acquisition, Investigation, Methodology, Project administration, Resources, Supervision, Validation, Writing – review & editing.

Declaration of Competing Interest

The authors declare that they have no known competing financial interests or personal relationships that could have appeared to influence the work reported in this paper.

Data availability

Data will be made available on request.

References

European Environment Agency https://www.eea.europa.eu/publications/covid-19-and-europe-s (Accessed: September 2021, Last Modified: March 2021).

European Environment Agency https://www.eea.europa.eu/signals/themes/air/air-quality-and-covid19/air-quality-and-covid19 (Accessed: September 2021, Last Modified: May 2021).

Apte, J.S., Messier, K.P., Gani, S., Brauer, M., Kirchstetter, T.W., Lunden, M.M., Marshall, M.M., Portier, C.J., Vermeulenand, R.C.H., Hamburg, S.P., 2017. High-resolution air pollution mapping with google street view cars: exploiting big data. Environ. Sci. Technol. 51, 6999–7008. https://doi.org/10.1021/acs.est.7b00891.

AQMesh https://www.aqmesh.com/products/aqmesh/ (Accessed: October 2022).

Barthelemy, M. The structure and dynamics of cities (Cambridge University Press, Cambridge, 2016). DOI: 10.1017/9781316271377.

Bassani, C., Vichi, F., Esposito, G., Montagnoli, M., Giusto, M., Lanniello, A., 2021. Nitrogen dioxide reductions from satellite and surface observations during COVID-19 mitigation in Rome (Italy). Environ. Sci. Pollut. Res. Int. 28, 22981–23004. https://doi.org/10.1007/s11356-020-12141-9.

Carcel-Carrasco, J., Pascual-Guillamon, M., Langa-Sanchis, J., 2021. Analysis of the effect of COVID-19 on air pollution: perspective of the Spanish case. Environ. Sci. Pollut. Res. Int. 28 https://doi.org/10.1007/s11356-021-13301-1.

Cerrato-Alvarez, M., Miro-Rodriguez, C., Pinilla-Gil, E., 2021. Effect of COVID-19 lockdown on air quality in urban and suburban areas of Extremadura, Southwest Spain: A case study in usually low polluted areas. Rev. Int. Contam. Amb. 37 https://doi.org/10.20937/RICA.54145.

Chadwick, E., Le, K., Pei, Z., Sayahi, T., Rapp, C., Butterfield, A.E., Kelly, K.E., 2021. Technical note: Understanding the effect of COVID-19 on particle pollution using low-cost sensor network. J. Aerosol Sci. 155, 105766 https://doi.org/10.1016/j.jaerosci.2021.105766.

Chen, Z., Hao, X., Zhang, X., Chen, F., 2021. Have traffic restrictions improved air quality? A shock from COVID-19. J. Clean. Prod. 279, 123622 https://doi.org/10.1016/j.jclepro.2020.123622.

Chicco, A., Diana, M., 2021. Air emissions impacts of modal diversion patterns induced by one-way car sharing: A case study from the city of Turin. Transp. Res. D Transp. Environ. 91, 102685 https://doi.org/10.1016/j.trd.2020.102685.

Chossiere, G.P., Xu, H., Dixit, H., Isaacs, H., Eastham, S.D., Allrogg, F., 2021. Air Pollution impacts of COVID-19-related containment measures. Sci. Adv. 7–21 https://doi.org/10.1126/sciadv.abe1178.

City of London, https://news.cityoflondon.gov.uk/air-pollution-in-the-city-of-london-drops-by-a-third-since-covid-19-lockdown/ (Accessed: September 2021).

Environmental Defense Fund. The Breathe London Footprint, 2020. https://c40.my.salesforce.com/sfc/p/#36000001Enhz/a/1Q000000gT7R/P78rbwoLSFKvYlZoL7fkrIzar2Soki7MPKgfrIdBFeM.

Gao, C., Li, S., Liu, M., Zhang, F., Achal, V., Tu, Y., Zhang, S., Cai, C., 2021. Impact of the COVID-19 pandemic on air pollution in Chinese megacities from the perspective of traffic volume and meteorological factors. Sci. Total Environ. 773, 145545 https://doi.org/10.1016/j.scitotenv.2021.145545.

Gensheimer, J., Chen, J., Turner, A. J., Shekhar, A., Wenzel, A., & Keutsch, F. N., 2021. What Are the Different Measures of Mobility Telling Us About Surface Transportation CO_2 Emissions During the COVID-19 Pandemic? J. Geophys Res. Atmos., 126(11), e2021JD034664. DOI: 10.1029/2021JD034664.

Gkatzelis, G.I., Gilman, J.B., Brown, S.S., Eskes, H., Gomes, A.R., Lange, A.C., McDonald, A.C., Peischl, J., Petzold, A., Thompson, C.R., Kiendler-Scharr, A., 2021. The global impacts of COVID-19 lockdowns on urban air pollution. Sci. Anthrop. 9, 00176. https://doi.org/10.1525/elementa.2021.00176.

Greater London Authority. *Air quality in London 2016-2020. London Environment Strategy: Air Quality Impact Evaluation*, 2020. https://www.london.gov.uk/sites/default/files/air_quality_in_london_2016-2020_october2020final.pdf.

Greater London Authority. *PM2.5 in London: Roadmap to meeting World Health Organization guidelines by 2030*, 2019. https://www.london.gov.uk/sites/default/files/pm2.5_in_london_october19.pdf.

Hudda, N., Simon, M.C., Patton, A.P., Durant, J.L., 2020. Reductions in traffic-related black carbon and ultrafine particle number concentrations in an urban neighborhood during the COVID-19 pandemic. Sci. Total Environ. 742, 140931 https://doi.org/10.1016/j.scitotenv.2020.140931.

Hodan, William M. and William R. Barnard. "Evaluating the Contribution of PM 2 . 5 Precursor Gases and Re-entrained Road Emissions to Mobile Source PM 2 . 5 Particulate Matter Emissions." (2004) , Environmental Protection Agency, Technical Report, https://www3.epa.gov/ttnchie1/conference/ei13/mobile/hodan.pdf.

Le, T., Wang, Y., Liu, L., Yang, J., Yung, Y.L., Li, G., Seinfeld, J.H., 2020. Unexpected air pollution with marked emission reductions during the COVID-19 outbreak in China. Science, 369-6504 704-706. DOI: 10.1126/science.abb7431.

Li, Q., Bou-Zeid, E., 2019. Contrasts Between Momentum and Scalar Transport Over Very Rough Surfaces. J. Fluid Mech. 880, 32–58. https://doi.org/10.1017/jfm.2019.687.

Liu, Y., Chen, H., Gao, J., Li, Y., Dave, K., Chen, J., Federici, M., Perricone, G., 2021. Comparative analysis of non-exhaust airborne particles from electric and internal combustion engine vehicles, J. Hazard. Mater., 420, 126626. DOI : 10.1016/j.jhazmat.2021.126626.

Liu, J., Lipsitt, J., Jerrett, M., Zhu, Y., 2021a. Decreases in Near-road NO and NO_2 Concentrations during the COVID-19 pandemic in California. Environ. Sci. Technol. Lett. 8–2, 161–167. https://doi.org/10.1021/acs.estlett.0c00815.

Llaguno-Munitxa, M. & Bou-Zeid, E., 2020. Sensing the environmental neighborhoods. In: Yuan P.F., Yao J., Yan C., Wang X., Leach N. (eds). Proceedings of the 2020 DigitalFUTURES CDRF-Springer. DOI: 10.1007/978-981-33-4400-6_12.

Llaguno-Munitxa, M., Bou-Zeid, E., 2018. Shaping buildings to promote street ventilation: a large-eddy simulation study. Urban Climate 26 (76–94), 9. https://doi.org/10.1016/j.uclim.2018.08.006.

Llaguno-Munitxa, M., Bou-Zeid, E., 2020a. Environmental neighborhoods and their spatial extent. Environ. Res. Lett. 15, 074034 https://doi.org/10.1088/1748-9326/ab8d7e.

Llaguno-Munitxa, M, Shu., X, Mistry, B., 2021. Multivariate analysis of the influence between building design and energy performance, socio-demographic metrics, and the intra-urban environment. J. Phys.: Conf. Ser., 2069 012056. DOI: 10.1088/1742-6596/2069/1/012056.

Breathe London. "Breathe London Technical Report: Pilot Phase (2018-2020)", 2020. https://www.globalcleanair.org/files/2021/05/BL-Pilot-Final-Technical-Report.pdf.

Breathe London https://www.breathelondon.org/ (Accessed: October 2022).

Marinello, S., 2021. The impact of the COVID-19 emergency on local vehicular traffic and its consequences for the environment: the case of the city of Reggio Emilia (Italy). Sustainability 13–118. https://doi.org/10.3390/su13010118.

Mayor of London, Healthy streets for London, 2017. http://content.tfl.gov.uk/healthy-streets-for-london.pdf.

Mittal, L., 2020. London Air Quality Network Summary Report 2020. https://www.londonair.org.uk/london/reports/2020_LAQN_Report.pdf.

Monks, P. Fine Particulate Matter (PM2.5) in the United Kingdom, 2012. https://uk-air.defra.gov.uk/assets/documents/reports/cat11/1212141150_AQEG_Fine_Particulate_Matter_in_the_UK.pdf.

Motlagh, N.H., Zaidan, M.A., Fung, P.L., Lagerspetz, E., Aula, K., Varjonen, S., Siekkinen, M., Rebeiro-Hargrave, A., Petäjä, T., Matsumi, Y., Kulmala, M., Hussein, T., Nurmi, P., Tarkoma, S., 2021. Transit pollution exposure monitoring using low-cost wearable sensors. Transp. Res. D Transp. Environ. 98, 102981 https://doi.org/10.1016/j.trd.2021.102981.

Nivergelt, Y., 1983. The concept of elasticity in economics. SIAM Rev. 25 (2), 261–265.

Oke, T.R., Mills, G., Christen, A., Voogt, J.A., 2017. Urban climates. Cambridge University Press.

Pearson, K., 1895. Notes on regression and inheritance in the case of two parents. Proc. Royal. Soc. Lond. 58, 240–242.

Ravindra, K., Singh, T., Biswal, A., Singh, V., 2021. Impact of COVID-19 lockdown on ambient air quality in megacities of India and implication for air pollution control strategies. Env Sci. Pollut. Res. Int. 28 (17), 21621–21632. https://doi.org/10.1007/s11356-020-11808-7.

Sahoo, P.K., Salomao, G.N., da Silva Ferreira Jr, J., Farias, D.L., Powell, M.A., Mittal, S.M., Garg, V.K., 2021. COVID-19 lockdown: a rare opportunity to establish baseline pollution level of air pollutants in a megacity, India. Int. J. Environ. Sci. and Technol., 18 1269-1286. DOI: 10.1007/s13762-021-03142-3.

Salma, I., Vorosmarty, M., Zeno Gyongyosi, A., Then, W., Weidinger, T., 2020. What can we learn about urban air quality with regard to the first outbreak of the COVID-19 pandemic? A case study from central Europe. Atmos. Chem. and Phys. 20–24 https://doi.org/10.5194/acp-20-15725-2020.

Sasidharan, M., Singh, A., Torbaghan, M.E., Parlikad, A.K., 2020. A vulnerability-based approach to human-mobility reduction for countering COVID-19 transmission in London while considering local air quality. Sci. Total Environ. 741, 14515. https://doi.org/10.1016/j.scitotenv.2020.140515.

Seinfeld, J.H. and Pandis, S.N., 2006. Atmospheric Chemistry and Physics: From Air Pollution to Climate Change. 2nd Edition, John Wiley & Sons, New York.

Timmers, V.R.J.H., Achten, P.A.J., 2016 . Non-exhaust PM emissions from electric vehicles. Atmos. Envon., 134, 10-17. DOI: 10.1016/j.atmosenv.2016.03.017 TomTom Move https://move.tomtom.com (Accessed: September 2021).

Tsakalidis, A., Krause, J., Julea, A., Peduzzi, E., Pisoni, E., Thiel, C., 2020. Electric light commercial vehicles: Are they the sleeping giant of electromobility? Transp. Res. D: Transp. Environ. 86, 102421 https://doi.org/10.1016/j.trd.2020.102421.

Venter, Z.S., Aunan, K., Chowdhury, S., Lelieveld, J., 2020. COVID-19 lockdowns cause global air pollution declines. PNAS 227 (32), 18984–18990. https://doi.org/10.1073/pnas.2006853117.

Wang, S., Ma, Y., Wang, Z., Wang, L., Chi, X., Ding, A., Yao, M., Li, Y., Li, Q., Wu, M., Zhang, L., Xiao, Y., Zhang, Y., 2021b. Mobile monitoring of urban air quality at high. Spatial resolution by low-cost sensors: impacts of COVID-19 pandemic lockdown. Atmos. Chem. Phys. 21, 7199–7215. https://doi.org/10.5194/acp-21-7199-2021.

Wang, J., Xu, J., Wang, S., He, S., He, P., 2021a. Heterogeneous effects of COVID-19 lockdown measures on air quality in Northern China. Appl. Energy 282, 116179. https://doi.org/10.1016/j.apenergy.2020.116179.

Wu, C.L., Wang, H.W., Cai, W.J., He, H.D., Ni, A.N., Peng, Z.R., 2021. Impact of the COVID-19 lockdown on roadside traffic-related air pollution in Shanghai. China. Build. Environ. 194, 107718 https://doi.org/10.1016/j.buildenv.2021.107718.

Xiang, J., Austin, E., Gould, T., Shirai, J., Liu, Y., Marshall, J., Seto, E., 2020. Impacts of the COVID-19 responses on traffic-related air pollution in a Northweastern US city. Sci. Total Environ. 747, 141325 https://doi.org/10.1016/j.scitotenv.2020.141325.

Yang, J., Bou-Zeid, E., 2019. Designing sensor networks to resolve spatio-temporal urban temperature variations: fixed, mobile or hybrid? Environ. Res. Let. 14, 074022 https://doi.org/10.1088/1748-9326/ab25f8.